Compensating complete loss of signal recognition particle during co-translational protein targeting by the translation speed and accuracy

Liuqun Zhao[a,b,c], Gang Fu[a,c], Yanyan Cui[a,c], Zixiang Xu[a,d], Dawei Zhang[a,b,c,d*]

[a]Tianjin Institute of Industrial Biotechnology, Chinese Academy of Sciences, Tianjin, China

[b]University of Chinese Academy of Sciences, Beijing, China

[c]Key Laboratory of Systems Microbial Biotechnology, Chinese Academy of Sciences, Tianjin, China.

[d]National Engineering Laboratory for Industrial Enzymes, Chinese Academy of Sciences, Tianjin, China.

Running Head: Translational control regulates protein targeting

[*]For correspondence. E-mail: zhang_dw@tib.cas.cn

ABSTRACT

Signal recognition particle (SRP) is critical for delivering co-translational proteins to the bacterial inner membrane. Previously, we identified SRP suppressors in *Escherichia coli* that inhibit translation initiation and elongation, which provides an insight into the mechanism of bypassing the requirement of SRP. Suppressor mutations tend to be located in regions that govern protein translation under evolutionary pressure. To verify this hypothesis, we re-executed the suppressor screening of SRP. Here we isolated a novel SRP suppressor mutation located in the Shine-Dalgarno sequence of S10 operon, which partially offset the targeting defects of SRP-dependent proteins. We found that the suppressor mutation slowed the translation rate of proteins, especially of inner membrane proteins, which could compensate for the targeting defects of inner membrane proteins via extending the time window of protein targeting. Furthermore, the fidelity of translation was decreased in suppressor cells, suggesting that the quality control of translation was inactivated to provide a survival advantage under the loss of SRP stress. Our results demonstrate that the inefficient protein targeting due to SRP deletion can be rescued through modulating translational speed and accuracy.

SUMMARY

The signal recognition particle (SRP)-dependent delivery pathway is essential for membrane protein biogenesis. Previously, we reported that SRP is nonessential in *Escherichia coli* and slowing translation speed plays a critical role in membrane protein targeting. Here we identified a novel SRP suppressor that is also involved in translation. We found that translation speed and accuracy regulate membrane protein targeting. A slowdown of translation speed extends the time window for protein targeting. Meanwhile, a moderate decrease in translation fidelity ensures a suitable translation speed for better cell growth. These results provide that translation control could be a practical way to compensate for the loss of SRP.

KEYWORDS: signal recognition particle, suppressor, translational control, co-translational protein targeting

67 **INTRODUCTION**

68 The signal recognition particle (SRP) is a highly conserved ribonucleoprotein complex
69 involved in co-translational targeting of the ribosome-nascent chain complex to the
70 endoplasmic reticulum of eukaryotes or the inner membrane of prokaryotes (1, 2).
71 Although the size and composition of SRP are variable in different species, the key
72 subunits of SRP are evolutionarily conserved (3). The *Escherichia coli* SRP is much
73 simpler than that in eukaryotes, as it contains an essential and highly conserved subunit
74 called the fifty-four homologue (Ffh), which is homologous to mammalian SRP54, and
75 a small stable 4.5S RNA, which is homologous to domain IV in the mammalian 7S SRP
76 RNA (4-6). The *E. coli* SRP components can replace their mammalian homologues to
77 mediate efficient co-translational protein targeting of mammalian proteins (4, 5). This
78 suggests that the subunit SRP54 and domain IV of the 7S SRP RNA form the core
79 conserved elements of SRP, and SRP is remarkably conserved from bacteria to
80 mammals. SRP is primarily responsible for delivering integral membrane proteins (7,
81 8). It recognizes hydrophobic transmembrane domains or signal sequences when they
82 emerge from the ribosome exit tunnel (9). Further, the nascent polypeptides must be
83 targeted by SRP in a limited time window before they lose their competence due to
84 aberrant aggregation (10, 11). Given the crowded cellular environment, it is challenging
85 to correctly translocate newly synthesized proteins from the cytosol to the membrane.

86 SRP is essential in all organisms (12), except for the eukaryote *Saccharomyces*
87 *cerevisiae* (13) and prokaryotes *Streptococcus mutans* (14) and *E. coli* (15). In these
88 cases, the global repression of protein synthesis is associated with the loss of SRP (13,

15, 16). However, the precise mechanism of this tolerance remains poorly understood (13-16). One of the best-understood mechanisms is slowing translation elongation rate that extends the time window for targeting translating ribosomes. Previous studies have demonstrated that slowing translation speed contributes to enhancing protein folding and targeting (17-19). In co-translational translocation, protein folding and targeting are inherently coupled to its elongation (20). The kinetic competition between protein translation elongation and targeting modulates the efficiency of the co-translational targeting pathway (17, 21). In eukaryotes, the Alu domain of SRP arrests nascent chain translation elongation during its targeting, which is thought to pause translation elongation until the targeting is completed (22, 23). Further, the Shine-Dalgarno-like sequence pauses translation before the second transmembrane domain exposed in *E. coli*, which facilitates the proper folding and targeting of membrane proteins (24). Thus, the translation elongation is at the center of protein folding and targeting.

In an earlier study, we identified SRP suppressors: two translation initiation factors IF2 and IF3, and a ribosomal protein RS3. The suppressor mutations decrease the translation initiation and elongation rate (15). There are two possible explanations for the slowing translation rate. First, it is possible that suppressor mutations directly inhibit the translation initiation and then decrease the translation elongation rate because the translation initiation rate is closely correlated with the elongation rate (25). Alternatively, the ribosome is a hub in protein homeostasis, which modulates protein translation and folding (19, 26). Here, we isolated an SRP suppressor located at the Shine-Dalgarno (SD) sequence of ribosome S10 operon that could affect ribosomes

111 biogenesis. We addressed how the suppressor regulates the translation process and
112 alleviates the fitness loss. Our results suggested that ribosome mutation suppressed the
113 loss of SRP, although the cell growth was severely inhibited and the targeting of SRP-
114 dependent proteins was not completely compensated. This SRP suppressor reduced
115 translation rate, especially of inner membrane proteins. Moreover, in response to SRP
116 deletion stress, the degree of mistranslation was increased to improve cell viability.
117 Overall, our results showed that mutations in the ribosome may contribute to protecting
118 cells from lethal damages caused by the loss of SRP.

119 **RESULTS**

120 **Identification suppressors of SRP.** Previous study in our laboratory demonstrated that
121 SRP suppressors were all associated with protein translation (15). To determine whether
122 suppressor mutations of SRP deletion were all mapped to chromosomal loci that
123 influence protein translation, we used the same suppressor approach as previously
124 described to screen SRP suppressors (15). We obtained another suppressor strain
125 MY1901 that could survive when SRP was deleted (Fig. 1A). The growth rate of
126 MY1901 was significantly reduced compared with that of wild-type strain MG1655,
127 suggesting that the MY1901 strain had a severe growth defect. We also found that a
128 longer lag time during the growth course of MY1901 than that of MG1655 (Fig. 1A),
129 indicating that the lag time before regrowth may provide ample time for the cell to adapt
130 to the absence of SRP. Whole-genome sequencing of the suppressor strain MY1901 and
131 the original strain MG1655 allowed us to identify the suppressor mutation site in the
132 SD sequence of ribosome S10 operon (Fig. 1B; Table S2). The S10 operon encodes 11

133 different ribosomal proteins and is responsible for protein synthesis (27). To determine
134 whether restoration of the wild-type alleles could revert to the wild-type strain, the Ffh
135 expression and reverting suppressor mutation to the wild-type allele in MY1901 strain
136 were carried out (Fig. 1C). The expression of Ffh markedly shortened the lag time and
137 increased the growth rate (Fig. 1D). Further, reverting the suppressor mutation to the
138 wild-type allele makes the growth rate of strain MY1901FS close to that of wild-type
139 strain MG1655 (Fig. 1D). Thus, the deletion of Ffh and suppressor mutation indeed
140 reduced cell growth. These results suggest that the mutation in the SD sequence of S10
141 operon contributes to the cell survival without SRP and this mutation is a novel
142 suppressor of SRP.

143 We hypothesized that the evolutionarily selective forces shaped the translation
144 process during screening suppressors in SRP-deletion cells. Thus, we tried to improve
145 cell growth through laboratory evolution. The strain MY1901 were analyzed by
146 continual subculture without any pressure over eighty rounds. The evolved strain
147 showed insignificant change in the growth rate but shorter lag time before regrowth and
148 an increased biomass compared with the initial strains (Fig. S1). The laboratory evolved
149 strains were sequenced and new changes in genes were identified (Table S2). In the
150 evolved strain MY1901, we found a mutation in the ribosomal protein S10 (rpsJ)
151 belonging to the S10 operon, confirming that the S10 operon plays an important role in
152 cell survival. Additionally, we obtained mutations in the DNA replication initiator
153 protein DnaA (28) and RNA polymerase rpoBC operon (29) (Table S2), which regulate
154 gene expression. Taken together, protein synthesis plays a critical role in suppressing

155 the loss of SRP.

156 **Effects of SRP suppressor on protein synthesis.** To examine the differences between
157 wild-type and mutant SD sequence, the mfold web server (30) was used to measure
158 mRNA structures of the S10 leader sequence containing the SD sequence. S10 leader
159 is required for the regulation of S10 operon (31). We found a 2.4 kcal mol^{-1} difference
160 in the minimum free energy of the thermodynamic ensemble of the predicted structure
161 of mutant SD compared to the wild-type SD (Fig. S2), suggesting that the S10 leader
162 with mutant SD was less stable. Because translation initiation is partially modulated by
163 the SD sequence (32), the effects of the mutant SD sequence on protein translation were
164 determined. The expression level of the green fluorescent protein (GFP) was used to
165 characterize protein translation levels in cells. Regardless of whether under the original
166 promoter P_{S10} or the arabinose inducible promoter P_{araBAD}, the expression level of GFP
167 with the mutated SD (SD*) was decreased (Fig. 2A), confirming that the suppressor
168 mutation weakened the binding of mRNA SD sequence to rRNA in ribosomes. This
169 result suggested that the translation initiation rate of S10 operon was reduced. To
170 examine whether the suppressor mutation decreases the expression levels of ribosomal
171 proteins, the whole-cell lysates proteome of strain MY1901 was analyzed (Data set
172 S1A). The expression level of each gene was normalized by that in wild-type strain
173 MG1655 (15). Unexpectedly, the levels of S10 operon and even the overall ribosomal
174 proteins were upregulated (Fig. 2B; Data set S1B). Given that the protein synthesis is
175 closely dependent on the ribosome content (33), there is a possibility that the protein
176 synthesis is enhanced in suppressor cells. However, the suppressor strain MY1901

177 showed a lower protein synthesis level because of a severe cell growth (Fig. 1A). Thus,
178 the increased pool of ribosomal proteins may be caused by the stalled ribosomes at the
179 translation initiation site, which are consistent with our previous study (15). Taken
180 together, although ribosomal protein biogenesis was increased, the protein synthesis
181 was reduced because of the inefficient translation.

182 **Translation speed and accuracy in suppressor cells.** Why did some ribosome
183 proteins accumulate in suppressor strain MY1901? One possibility is that ribosome
184 slowly translates mRNAs in suppressor cells. To test this possibility, we carried out
185 polysome profiling, which could detect various defects of translation. The polysome
186 profile of suppressor cells was changed relative to wild-type cells (Fig. 3A). The 30S
187 to 50S (30S/50S) ratio was not significantly altered in suppressor and wild-type strains,
188 but the 30S and 50S peaks of suppressor cells were higher than that of wild-type cells
189 (Fig. 3A), indicating an increase in the proportion of free subunits. The 70S peak of the
190 wild-type cells was almost indistinguishable from that of suppressor cells, suggesting
191 that some 70S ribosomes may pause at the translation initiation. We observed that the
192 polysome to 70S monosome (P/M) ratio was decreased in suppressor cells (Fig. 3A),
193 suggesting that translation elongation was inhibited in suppressor cells. Thus, the
194 suppressor mutation plays a role in protein translation. Translation can be divided into
195 four phases: initiation, elongation, termination, and ribosome recycling (34). We next
196 compared the protein abundances of translation associated factors via whole-cell lysates
197 proteome analysis. Ribosome recycling factor (RRF) and elongation factor-G (EF-G)
198 are involved in ribosome recycling (35). The expression of RRF and EF-G was

199 downregulated in suppressor strain (Fig. 3B; Data set S1B), indicating that the ribosome
200 recycling was reduced, which may be caused by slowing translation in suppressor cells.
201 Although the expression of release factors mediating translation termination was
202 upregulated, the efficiency of translation termination at three stop codons was only
203 slightly increased (Fig. 3B and C). This data showed that the translation termination
204 rate was not significantly impacted in suppressor cells. We observed that the expression
205 level of elongation factors in suppressor cells was inconsistent and changed little
206 compared to that in wild-type cells (Fig. 3B; Data set S1B). To exactly examine the
207 efficiency of translation elongation, we measured its fidelity and speed through
208 experiments. In strain MY1901, we observed a marked increase in translational
209 frameshifting readthrough relative to that in wild-type strain (Fig. 3D), thus the fidelity
210 of translation elongation was decreased. Additionally, a LacZ induction assay was used
211 to measure the translation elongation speed (36). We used a cytoplasmic protein FusA
212 and an inner membrane protein MsbA to define the level of translation elongation rates
213 (Fig. S3). When cells were grown at the same rich growth media (Glucose + cAA), the
214 growth rates of wild-type and suppressor cells were approximately 1.0 h^{-1}(15) and 0.6
215 h^{-1}, respectively (Fig. S3A; Table S3). As expected, the translation elongation rate of
216 suppressor cells was markedly decreased compared with that of wild-type cells (Fig.
217 3E; Fig. S3B to F). As the translation elongation closely depends on growth rate (37),
218 we further reduced the growth rate of wild-type cells to 0.6 h^{-1} that was similar to that
219 of suppressor cells (Fig. S3A). The elongation rate of the MsbA in suppressor cell was
220 reduced by approximate 2.0 aa s^{-1} (amino acids per second) compared with that in wild-

221 type cells, but the elongation rate of the FusA was similar in both wild-type and
222 suppressor cells (Fig. 3E; Fig. S3B toD). We also observed that the elongation rate of
223 MsbA was slower than that of FusA (Fig. 3E; Fig. S3B to F), which is consistent with
224 the issue that the translation speed of inner membrane proteins is slowed down during
225 targeting, but not that of cytoplasmic proteins (24). These data suggested that the effect
226 of selectively reducing translation elongation rate of inner membrane proteins was
227 enhanced in suppressor cells. For the expression of translation initiation factors in
228 suppressor cells, IF1 and IF3 were downregulated but IF2 was upregulated (Fig. 3B).
229 Given that IF2 accelerates ribosomal subunit joining, whereas IF1 and IF3 slowed down
230 subunit association (38, 39), the capacity of formation of 70S initiation complex may
231 not be significantly impaired although cells showed severe defects in growth. We next
232 examined the translation initiation rate by a computational model called the
233 homogeneous ribosome flow model (HRMF), in which the translation elongation rate
234 was assumed to be constant (40). The translation initiation rate can be estimated by the
235 measurable translation rate and elongation rate (Table S4). The translation initiation
236 rate in suppressor cells showed similar trend to the translation elongation rate. The
237 initiation rate of FusA was not markedly changed in the suppressor and wild-type cells
238 when grown at the same growth rate (Fig. 3F). However, the inner membrane protein
239 MsbA had a slower translation initiation rate in suppressor cells than that in wild-type
240 cells when grown at the same growth rate (Fig. 3F). These results suggested that the
241 translation initiation rate was selectively decreased in suppressor cells. As translation
242 initiation factors play a vital role in translation initiation fidelity (39), we addressed

243 whether the suppressor was detrimental to the fidelity of start codon selection and
244 initiator tRNA binding. We changed the start codon of GFP from AUG to GUG, UUG,
245 AUA and AUC and the initiator tRNA codon of GFP from AUG: CAU to UAG: CUA,
246 CAC: GUG and UAC: GUA. We measured the GFP fluorescence of these GFP variants
247 in the wild-type and suppressor cells. We observed that the fidelity of translation
248 initiation in suppressor cells was decreased at different levels compared with that in
249 wild-type cells (Fig. 3G), indicating that suppressor mutation may impair the fidelity
250 of translation initiation. Taken together, the suppressor cell trades translation speed and
251 accuracy for cell survival in the absence of SRP.

252 **SRP-dependent protein targeting in suppressor cells.** In *E. coli*, most inner
253 membrane proteins are delivered by the co-translational SRP pathway (41). In principle,
254 SRP-dependent proteins are not properly targeted to the bacterial cytoplasmic
255 membrane after Ffh depletion (42, 43). To test whether the suppressor mutation could
256 suppress protein targeting defects, we first examined cell morphological changes by
257 scanning electron microscopy (SEM) and transmission electron microscopy (TEM).
258 SEM images showed that suppressor strain MY1901 still had typical rod morphology
259 but had rougher surface relative to the wild-type strain MG1655 (Fig. 4A). TEM images
260 showed that suppressor strain MY1901 retained cell wall integrity but had damaged
261 inner membrane structure (Fig. 4A). MY1901 displayed a significant detachment of the
262 inner membrane from the outer membrane (Fig. 4A). Thus, the suppressor mutation
263 partially offsets the effects of the loss of SRP pathway on inner membrane protein
264 translocation. To gain insight into the localization of inner membrane proteins, we

265 performed proteomic analysis of inner membrane proteins in strains wild-type
266 MG1655(15) and suppressor MY1901 (Data set S1C). The *E. coli* strain HDB51 was
267 used as a control, in which the expression of Ffh was induced by arabinose (44).
268 Depleted Ffh can be obtained after several hours of incubation in the presence of
269 glucose, thus yielding the SRP^-strain (45). The inner membrane proteome analysis of
270 SRP^- was also conducted (Data set S1C). According to the previous study, we identified
271 262 SRP-dependent inner membrane proteins (15). Since the completely untargeted
272 inner membrane proteins would aggregate or misfold in cytoplasm, the detected inner
273 membrane proteins by inner membrane mass spectrometry analysis are primary in their
274 folded and targeted state. We found that targeting levels of many identified SRP-
275 dependent inner membrane proteins in both MY1901 and SRP^- cells were higher than
276 their targeting levels in wild-type cells (Fig. 4B; Data set S1D), indicating that these
277 inner membrane proteins can target to the cytoplasmic membrane in the absence of SRP,
278 which is consistent with the previous study that the only part of the inner membrane
279 protein targeting was completely inhibited when SRP is inefficient (42). We also found
280 that more proteins were successfully targeted in MY1901strain than in SRP^- strain (Fig.
281 4B), suggesting that the suppressor mutation indeed plays a role in inner membrane
282 protein targeting without SRP. FtsQ is an SRP-dependent protein, which is often used
283 as a model protein for studying SRP-mediated protein targeting (17, 46). However, the
284 targeting of FtsQ was not significantly inhibited in strains SRP^- and MY1901 (Fig. 4B;
285 Data set S1D). This may be explained by the fact that FtsQ is a single-spanning
286 membrane protein that is easily targeted to the membrane (15, 47). To confirm this

287 result, we examined the targeting level of FtsQ by protein biotinylation (17, 48, 70).
288 The Avi-tag was fused to the periplasmic domain of the targeted proteins. The
289 biotinylated proteins would be the untargeted proteins in which the periplasmic
290 domains are exposed in the cytosol. Thus, the protein biotinylation can be used for
291 protein targeting assay. As expected, FtsQ can target to the inner membrane in all
292 different cells (Fig. 4C), which confirmed the prediction of proteomic analysis (Fig.
293 4B). We also found that the targeting levels of the SRP-independent protein EspP in all
294 strains were similar (Fig. 4C), suggesting that the targeting of SRP-independent
295 proteins was not affected by the loss of SRP. Thus, the suppressor enables SRP-
296 dependent protein targeting which did not occur at the cost of failed targeting of SRP-
297 independent proteins.

298 **DISCUSSION**

299 Co-translational protein targeting by SRP is an essential and conservative pathway that
300 delivers most inner membrane proteins to their correct subcellular destinations (3).
301 Early work revealed that SRP was not essential in *E. coli* when the translation initiation
302 and elongation rate were decreased (15). Isolation of suppressors is a useful strategy to
303 provide insight into certain molecular mechanisms by suggesting which cellular
304 component is involved in an inefficient process (49). The SRP suppressors involved in
305 protein translation initiation have been identified before, and these suppressors directly
306 affect the translation process (15). In this study, we obtained an SRP suppressor
307 associated with protein translation too. Additionally, the expression of heat shock
308 response related chaperones and proteases was not upregulated (Fig. S4A; Data set

309 S1B), suggesting that the heat shock response plays little role in compensating the loss
310 of SRP, which is consistent with the previous study (15). In strain MY1901, the
311 expression of SecA was not affected and other transport machinery components such
312 as SecYEG-YajC-SecDF, YidC, and FtsY showed a decreased level relative to those in
313 the wild-type strain (Fig. S4B; Data set S1E). Moreover, the expression level of these
314 components was similar in strains MY1901 and SRP$^-$ (Fig. S4B; Data set S1E). These
315 results suggest that protein transport machinery components were not likely involved
316 in protein targeting without SRP. Since the translation consumes a large amount of
317 energy, it is important to properly regulate the translation (50). However, there is
318 another possibility that the suppressor mutation may indirectly interfere with the
319 general translation process, and any strategies inhibiting translation can offset the
320 missing SRP. To exclude this possibility, we added a low level of chloramphenicol that
321 is well-known to block translation elongation into the medium of SRP$^-$ cells. We found
322 that chloramphenicol did not suppress cell growth defects in the absence of SRP (Fig.
323 S5), thus simply decreasing protein synthesis could not suppress the defects of SRP
324 deletion, which is inconsistent with the previous result that chloramphenicol suppresses
325 the SecY mutant (49). Together with the previous study (15), the SRP suppressors tend
326 to be identified in translation machinery.

327 Consistent with the previous observation (15), we observed that deletion of SRP
328 led to inefficient protein synthesis, suggesting a close relationship between protein
329 synthesis and translocation. Although the translation was repressed in strain
330 MY1901(Fig. 3E and F), the ribosomal protein expression was upregulated (Fig. 2B)

331 and the 30S and 50S ribosomal subunits were accumulated (Fig. 3A). This led to the
332 belief that the ribosomes may be inactive and accumulate in the cytosol. Consistent
333 with the earlier report (15), we observed that the assembly of 70S particles was not
334 significantly impaired (Fig. 3A). Thus, the 70S ribosomes initiation complex formation
335 process was not inhibited. Given that the protein translation initiation was impeded (Fig.
336 3E and F), we speculated that this impediment was due to the stalled initiation-like 70S
337 ribosome complex. However, we observed that the initiation time of translation was
338 constant in wild-type and suppressor cells under different growth rates (Table S3), thus
339 the initiation pausing can be negligible in suppressor cells and the suppressor mutation
340 did not affect the translation initiation process. Considering the translation elongation
341 rate is dependent on the growth rate (37), the growth defect may directly play a big role
342 in inhibiting translation elongation of membrane proteins. However, this possibility can
343 be excluded, because suppressor cells were grown under the rich nutrient condition that
344 can supply enough macromolecular for ribosomal synthesis and translation elongation,
345 and the cell growth could not automatically decrease (37, 51). Moreover, under the
346 same growth rate, the elongation rate of inner membrane protein in the suppressor cells
347 was also decreased relative to that in the wild-type cells (Fig. 3E). As the level of protein
348 translation and the growth rate is closely interweaved (51) and the translation
349 elongation plays a critical role in protein homeostasis that is important for cell growth
350 (52, 53), it is most likely that the cell growth rate depends on the level of elongation
351 rate and the slowing elongation rate are caused by the suppressor mutation. Increasing
352 evidence has supported the notion that the translation elongation of nascent polypeptide

353 regulates the targeting of SRP-dependent proteins (17, 21), thus decreasing elongation
354 rate contributes to the survival of SRP deletion cells. Interestingly, relative to wild-type
355 cells, the reduction level of translation rate of the cytoplasmic protein FusA was less
356 than that of the inner membrane protein MsbA in suppressor cells (Fig. 3E and F).
357 Hence, the suppressor mutation may be biologically favored to reduce the translation
358 of inner membrane proteins, which may be beneficial to cell fitness. Decreasing
359 translation elongation rate plays a critical role in suppressing the loss of SRP by
360 extending the time window for protein targeting (15). SRP binds to the ribosome-
361 nascent chain complex when the N-terminus of the first TMD is exposed from the
362 ribosome. The maximal SRP binding site is 55 amino acids from the ribosomal peptidyl
363 transferase center in *E. coli* (54). Assuming that ~30 amino acids can fit into the
364 ribosome exit tunnel (55), 25 residues would be exposed outside the tunnel. At a
365 translation elongation rate of ~15 aa s^{-1} in rapid growth conditions (15), the maximum
366 time required for protein localization is ~2 s (Fig. 5). Thus, with the help of SRP, most
367 translating ribosomes move to the membrane within this period in *E. coli*. Without SRP,
368 suppressors showed the translation elongation rate to ~11 aa s^{-1}(Fig. 3E; Table S3),
369 which also provides ~2 s for nascent chains of 55 amino acids to target to the inner
370 membrane (Fig. 5). However, it is not likely that nascent chains successfully target to
371 the membrane within ~2 s without SRP. To get a longer time to find the membrane, the
372 length of translating nascent chains is more likely longer than 55 amino acids. However,
373 the nascent chain cannot exceed a specific length as aggregation would prevent protein
374 from being targeted (10, 11), and this specific length is called the critical length (L) for

375 targeting. Proteins with fewer transmembrane domains (TMDs) or longer first loop
376 length have a longer critical length (15). Furthermore, if the nascent chain exceeds a
377 critical length of ~140 amino acids, it becomes translocation-incompetent (10, 11). In
378 suppressor cells, the upper limit of the critical time for protein targeting would be ~10
379 s (Fig. 5). If the targeting time of some SRP-dependent proteins exceeds 10 s, these
380 proteins would not be targeted to the inner membrane in suppressor cells. Thus, the
381 suppressor extends the time window to ~2-10 s (Fig. 5). Taken together, this model
382 shows that SRP greatly shortened the protein targeting time up to 8 s, which minimizes
383 the cost of targeting and maintains a fast growth. Furthermore, we showed that the
384 translation fidelity was decreased in suppressor cells (Fig. 3D and G). Earlier work
385 revealed that mistranslation can provide a growth advantage in response to stress (56).
386 Hence, the suppressor mutation may inactive the translation quality control mechanism
387 to alleviate the stress response and maintain cell growth. Overall, our data suggest that
388 in response to the deletion of SRP, suppressor cells attenuate translation elongation to
389 give the translating ribosomes more time to find and target to the inner membrane.
390 Additionally, suppressor mutation selectively permits SRP-dependent proteins
391 translation and reduced the fidelity of translation, which is vital to cell survival.

392 As expected, the suppressor mutation can partially offset the defective targeting of
393 inner membrane proteins (Fig. 4B), which is consistent with the previous result (15).
394 Furthermore, we found that in the SRP-depletion strain SRP^{-}, many proteins can
395 successfully target to the inner membrane (Fig. 4B). However, proper localization of
396 these proteins cannot bypass the requirement of SRP (57). We speculated that the

397 proteins that can be correctly located in suppress strain MY1901 but not in SRP-
398 depletion strain SRP⁻ may be responsible for cell survival. We hypothesized that
399 specific membrane protein targeting defects can block the essential cellular process,
400 which would be responsible for the loss of cell viability. Among these localization
401 defective proteins, only one protein PgsA is essential for *E. coli* (Data set S1F). PgsA
402 catalyzes the step in the synthesis of the acidic phospholipids that are considered to be
403 indispensable in multiple cellular processes (58, 59). We speculated that mislocalization
404 of PgsA may inhibit cell growth. Furthermore, in SRP⁻ strain, some transportation
405 associated proteins (AsmA, Bcr, PheP, YbaL, and YidE) did not successfully target to
406 the inner membrane (Data set S1F), which would impair membrane traffic and decrease
407 energy production. Further studies are needed on the protein targeting defects that
408 determine whether cells devoid of SRP will survive.

409 **MATERIALS AND METHODS**

410 **Bacterial strains, plasmids and media.** All bacterial strains, plasmids and primers
411 used in this study are listed in Table S1. *E. coli* K-12 MG1655 derivative strains were
412 grown either in LB medium or on LB agar at the indicated temperature. *E. coli* HDB51
413 strain in which the expression of Ffh is under the control of an arabinose inducible
414 promoter, were grown in LB medium containing 0.2% arabinose (44). The SRP
415 suppressor strain MY1901 was isolated and validated as previously described. The
416 antibiotics kanamycin, gentamycin, ampicillin, and chloramphenicol were used at a
417 concentration of 50, 10, 100, and 200 μg ml^{-1}, respectively. The *lac*, *trc* and *tac*
418 promoters were induced with 0.02 mM isopropyl-β-D-1-thiogalactopyranoside (IPTG).

419 The *araBAD* promoter was induced with 0.2% arabinose.

420 **Measurement of cell growth.** The bacterial growth curves and growth rates were
421 estimated as previously predicted (15). For bacterial growth under oxidative and
422 osmotic stress, overnight cultures were diluted into liquid LB media containing 2 mM
423 or 8 mM H_2O_2 and 2.5% or 5% NaCl, respectively. For the thermal stress experiment,
424 the medium was chilled to 30°C or heated to 42°C before inoculation.

425 **Polysome analysis, cell ultrastructure and proteomic analysis.** Strains were grown
426 at 37°C at the early-exponential growth in LB medium and harvested by centrifugation
427 (15). Polysome analysis was performed as described (60, 61). The scanning electron
428 microscopy (SEM) and transmission electron microscopy (TEM) analyses were carried
429 out as described previously (15). The whole-cell lysates and inner membrane proteins
430 of strains MY1901 and SRP^- were isolated and analyzed by liquid chromatography-
431 tandem mass spectrometry (LC-MS/MS) as described (15, 62-64), with modifications.
432 For seed culture, the strain MY1901 or HDB51was inoculated in LB medium at 37°C
433 overnight and the strain HDB51 was grown under the addition of 0.2% arabinose. The
434 overnight culture of MY1901 was diluted into the fresh LB medium with an initial
435 OD_{600} of 0.02-0.03. Strain MY1901 was harvested in the mid-exponential phase. The
436 overnight culture of HDB51 was washed for three times with fresh LB medium and
437 then incubated in LB with addition of 0.2% glucose with an initial OD_{600} of 0.03-0.04
438 for several hours, yielding the SRP^- strain. This strain was harvested when entering the
439 stationary phase. Three sample replicates were prepared by performing collection of
440 cells from independent cultures. We used the Filter-Aided Sample Preparation (FASP)

441 strategy for proteome analysis (63). The inner membrane fraction was separated by
442 sucrose gradient (64). Then, the inner membrane was chemically treated by Na_2CO_3
443 and KCl to remove peripherally associated proteins (15). The MS sample of inner
444 membrane proteins was prepared by surface proteolysis (64). The sample was
445 characterized by sequential window acquisition of all theoretical spectra (SWATH)
446 analysis (65). The LC-MS/MS analysis was performed according to the previous study
447 (15). The obtained data were normalized by the median scale normalization (MedScale)
448 method (66).

449 **β-galactosidase assay.** The β-galactosidase activity was assayed as previously
450 described (67). Cells were grown in LB medium supplemented with 50 μg ml^{-1}
451 kanamycin at 37°C. Protein induction was performed when MG1655Δ*lacZ* and
452 MY1901Δ*lacZ* were grown to OD_{600} of 0.6-0.8 and 0.4-0.5, respectively. Two hours
453 later the cultures were harvested and assayed. β-galactosidase activity from the plasmid
454 encoding wild-type LacZ was used for normalization.

455 **Measurements of translation efficiency and initiation fidelity.** To determine the
456 effects of mutated SD sequence on protein translation efficiency, we constructed
457 plasmids carrying the *gfp* gene with the wild-type SD and suppressor mutation SD*
458 under the promoter P_{S10} or P_{araBAD}. To analyze the translation initiation fidelity, a set of
459 GFP variants were generated in which the start codon (AUG) or the initiator tRNA was
460 replaced with different non-canonical start codons and non-initiator tRNAs codons.
461 Several non-canonical start codons (GUG, UUG, AUA and AUC) and non-initiator
462 tRNAs codons (UAG: CUA, CAC: GUG and UAC: GUA) were used as potential start

463 codons and initiator tRNAs codons, respectively. *E. coli* cells were grown in 300 μl of
464 LB medium with necessary antibiotics in a 96-well deep well culture plate at 37°C
465 overnight followed by transferring and cellular fluorescence measurements (68). For
466 detecting the effects of Shine-Dalgarno (SD) sequence on translation efficiency and the
467 fidelity of translation initiation, the non-expression strains containing empty vectors
468 pJH30, pJH31 and pTrc99K lacking a reporter gene were used as controls. OD_{600} was
469 measured to estimate culture density, followed by fluorescence (excitation=488 nm,
470 emission=520 nm). Assays were carried out from six independent colonies. For the
471 initiation fidelity assay, the fluorescence intensity from the plasmid encoding mutant
472 GFP was normalized against the fluorescence intensity of wild-type or suppressor
473 strains containing plasmid encoding wild-type GFP.

474 **Measurements of translation rates.** Translation elongation rates were measured as
475 described previously (36, 37, 69). For seed culture, MG1655Δ*lacZ* and
476 MY1901Δ*lacZ*Δ*cat* cells were cultured in LB medium at 37°C for several hours, then
477 cultures were collected and washed with fresh MOPS medium. To make strains grow
478 well, MG1655Δ*lacZ* and MY1901Δ*lacZ*Δ*cat* it was grown in rich Glucose + cAA (0.2%
479 glucose + 0.2% casamino acids) MOPS medium overnight as the pre-culture. The
480 experiment culture was performed with an initial OD_{600} of 0.04-0.05. The subsequent
481 collection and measurement methods were performed as previously described (15). The
482 translation elongation rate was measured based on the LacZα induction assay. The
483 translation time of first newly synthesized LacZα, T_{α}, was estimated by measuring the
484 LacZα induction kinetics. The translation time of the first newly synthesized

485 LacZα fused protein (FusA-LacZα or MsbA- LacZα), T_{total}, was obtained by Schleif
486 plot of the induction curve. The initiation time, T_{init}, equals T_{α}–{90/[L/(T_{total}–T_{α})]},
487 where 90 is the 90 aa LacZα fragment and L is the length of the LacZα fusion protein
488 (containing 10 aa linker). The translation elongation rate equals (L+90)/(T_{total}–T_{init}).
489 When MY1901Δ*lacZ*Δ*cat* grew in Glucose + cAA medium, the growth rate of it was
490 about 0.6 h^{-1}. To eliminate the cell growth effect on translation elongation rate, the wild-
491 type strain MG1655Δ*lacZ* was grown in Glycerol + NH_4Cl (0.2% glycerol + 10 mM
492 NH_4Cl) MOPS medium and the growth rate was similar to 0.6 h^{-1}. The measurement of
493 the elongation rate of MG1655Δ*lacZ* with the growth rate 0.6 h^{-1} was performed
494 similarly to that of MY1901Δ*lacZ*Δ*cat*. Translation initiation rate was estimated by a
495 computational model homogeneous ribosome flow model (HRFM) (40, 70, 71). Based
496 on the measured translation rate and elongation rate, the initiation rate can be calculated
497 (15).

498 **Protein targeting assay *in vivo*.** The biotinylation of proteins has been successfully
499 applied to SRP-dependent protein targeting *in vivo* (17, 48). *E. coli* enzyme biotin ligase
500 (BirA) can specially ligate biotin to a 15-amino acid peptide (GLNDIFEAQKIEWHE)
501 termed the Avi-tag (72). The BirA and Avi-tagged proteins were co-expressed for
502 biotinylation. Cells were co-transformed with recombinant vectors p15A-birA and
503 pJH29-EspP/FtsQ/LacZ-Avi and grown overnight at 37°C. Then overnight cultures
504 were washed and diluted into 30 mL fresh LB medium at an initial OD_{600} of 0.02. For
505 HDB51, the overnight culture that grown in LB medium with 0.2% arabinose was
506 washed and diluted into 30 mL fresh LB medium at an initial OD_{600} of 0.02 with or

without arabinose to construct SRP^+ and SRP^- cells, respectively. When cultures reached an OD_{600} ~0.4-0.5 (SRP^- cells were cultured for 2-3 h), protein expression was induced by 0.5 mM IPTG, and 100 μM biotin was also added at this point. After 3 h of cultivation, cells were harvested by centrifugation. For Ffh depletion, 0.2% glucose was added 2 h before harvesting of cells. Then the samples were analyzed by SDS-PAGE and immunoblotting. Biotinylated proteins were detected by streptavidin-HRP and the total amount of protein was detected by anti-FLAG antibody. Detection was performed by the DAB substrate kit (Thermo Scientific, USA).

Acknowledgments

We thank Dr. Manlu Zhu (Central China Normal University) for plasmid pKUT15-fusA-lacZα, Dr. Changhao Bi (TIB, CAS) for plasmid pRed_Cas9_ΔpoxB300, Dr. Harris D Bernstein (NIH) for strain HDB51 and plasmid pJH29 and Dr. Zhidan Zhang (TIB, CAS) for help with mass spectrometry. This work was supported by the National Key R&D Program of China (2020YFA0907800) and Tianjin Synthetic Biotechnology Innovation Capacity Improvement Project (TSBICIP-KJGG-004-03 and TSBICIP-KJGG-006).

Conflict of interest

The authors declare no conflict of interest.

Author contributions

LZ, GF and DZ designed the experiments. LZ and YC performed experiments. LZ, YC, and ZX analyzed the data. LZ and DZ wrote the manuscript.

REFERANCES

1. Walter P, Johnson AE. 1994. Signal sequence recognition and protein targeting to the endoplasmic reticulum membrane. Annu Rev Cell Biol 10:87–119.
2. Pool MR. 2005. Signal recognition particles in chloroplasts, bacteria, yeast and mammals. Mol Membr Biol 22:3–15.
3. Saraogi I, Shan SO. 2014. Co-translational protein targeting to the bacterial membrane. Biochim Biophys Acta 1843:1433–1441.
4. Bernstein HD, Zopf D, Freymann DM, Walter P. Functional substitution of the signal recognition particle 54-kDa subunit by its Escherichia coli homolog. Proc Natl Acad Sci U S A 90:5229–5233.
5. Powers T, Walter P. 1997. Co-translational protein targeting catalyzed by the Escherichia coli signal recognition particle and its receptor. EMBO J 16:4880–4886.
6. Regalia M, Rosenblad MA, Samuelsson T. 2002. Prediction of signal recognition particle RNA genes. Nucleic Acids Research 30:3368–3377.
7. Zhang X, Shan SO. 2014. Fidelity of cotranslational protein targeting by the signal recognition particle. Annu Rev Biophys 43:381–408.
8. Ulbrandt ND, Newitt JA, Bernstein HD. 1997. The E. coli signal recognition particle is required for the insertion of a subset of inner membrane proteins. Cell 88:187–196.
9. Ng DT, Brown JD, Walter P. 1996. Signal sequences specify the targeting route to the endoplasmic reticulum membrane. J Cell Biol 134:269–278.

553 10. Siegel V, Walter P. 1988. The affinity of signal recognition particle for
554 presecretory proteins is dependent on nascent chain length. EMBO J 7:1769–
555 1775.
556 11. Flanagan JJ, Chen JC, Miao Y, Shao Y, Lin J, Bock PE, Johnson AE. 2003.
557 Signal recognition particle binds to ribosome-bound signal sequences with
558 fluorescence-detected subnanomolar affinity that does not diminish as the
559 nascent chain lengthens. J Biol Chem 278:18628–18637.
560 12. Akopian D, Shen K, Zhang X, Shan SO. 2013. Signal recognition particle: an
561 essential protein-targeting machine. Annu Rev Biochem 82:693–721.
562 13. Mutka SC, Walter P. 2001. Multifaceted physiological response allows yeast to
563 adapt to the loss of the signal recognition particle-dependent protein-targeting
564 pathway. Mol Biol Cell 12:577–588.
565 14. Kremer BH, van der Kraan M, Crowley PJ, Hamilton IR, Brady LJ, Bleiweis
566 AS. 2001. Characterization of the sat operon in Streptococcus mutans: evidence
567 for a role of Ffh in acid tolerance. J Bacteriol 183:2543–2552.
568 15. Zhao L, Cui Y, Fu G, Xu Z, Liao X, Zhang D. 2020. Signal recognition particle
569 suppressor screening reveals the regulation of membrane protein targeting by
570 the translation rate. mBio 11: e02373-20.
571 16. Hasona A, Zuobi-Hasona K, Crowley PJ, Abranches J, Ruelf MA, Bleiweis AS,
572 Brady LJ. 2007. Membrane composition changes and physiological adaptation
573 by Streptococcus mutans signal recognition particle pathway mutants. J
574 Bacteriol 189:1219–1230.

575 17. Zhang D, Shan SO. 2012. Translation elongation regulates substrate selection
576 by the signal recognition particle. J Biol Chem 287:7652–7660.
577 18. Siller E, DeZwaan DC, Anderson JF, Freeman BC, Barral JM. 2010. Slowing
578 bacterial translation speed enhances eukaryotic protein folding efficiency. J Mol
579 Biol 396:1310–1318.
580 19. Sherman MY, Qian SB. 2013. Less is more: improving proteostasis by
581 translation slow down. Trends Biochem Sci 38:585–591.
582 20. du Plessis DJ, Nouwen N, Driessen AJ. 2011. The Sec translocase. Biochim
583 Biophys Acta 1808:851–865.
584 21. Chartron JW, Hunt KC, Frydman J. 2016. Cotranslational signal-independent
585 SRP preloading during membrane targeting. Nature 536:224–228.
586 22. Walter P, Blobel G. 1981. Translocation of proteins across the endoplasmic
587 reticulum III. Signal recognition protein (SRP) causes signal sequence-
588 dependent and site-specific arrest of chain elongation that is released by
589 microsomal membranes. J Cell Biol 91:557–561.
590 23. Mason N, Ciufo LF, Brown JD. 2000. Elongation arrest is a physiologically
591 important function of signal recognition particle. EMBO J 19:4164–4174.
592 24. Fluman N, Navon S, Bibi E, Pilpel Y. 2014. mRNA-programmed translation
593 pauses in the targeting of E. coli membrane proteins. Elife 3:e03440.
594 25. Riba A, Di Nanni N, Mittal N, Arhné E, Schmidt A, Zavolan M. 2019. Protein
595 synthesis rates and ribosome occupancies reveal determinants of translation
596 elongation rates. Proc Natl Acad Sci U S A 116:15023–15032.

26. Pechmann S, Willmund F, Frydman J. 2013. The ribosome as a hub for protein quality control. Mol Cell 49:411–421.

27. Zengel JM, Lindahl L. 1994. Diverse mechanisms for regulating ribosomal protein synthesis in Escherichia coli. Prog Nucleic Acid Res Mol Biol 47:331–370.

28. Hughes P, Landoulsi A, Kohiyama M. 1988. A novel role for cAMP in the control of the activity of the E. coli chromosome replication initiator protein, DnaA. Cell 55:343–350.

29. Ishihama A, Fukuda R. 1980. Autogenous and post-transcriptional regulation of RNA polymerase synthesis. Mol Cell Biochem 31:177–196.

30. Zuker M. 2003. Mfold web server for nucleic acid folding and hybridization prediction. Nucleic Acids Res 31:3406–3415.

31. Allen T, Shen P, Samsel L, Liu R, Lindahl L, Zengel JM. 1999. Phylogenetic analysis of L4-mediated autogenous control of the S10 ribosomal protein operon. J Bacteriol 181:6124–6132.

32. Yang C, Hockenberry AJ, Jewett MC, Amaral LAN. 2016. Depletion of Shine-Dalgarno Sequences Within Bacterial Coding Regions Is Expression Dependent. G3 (Bethesda) 6:3467–3474.

33. Scott M, Gunderson CW, Mateescu EM, Zhang Z, Hwa T. 2010. Interdependence of cell growth and gene expression: origins and consequences. Science 330:1099–1102.

34. Rodnina MV. 2018. Translation in Prokaryotes. Cold Spring Harb Perspect Biol

10:a032664.

35. Prabhakar A, Capece MC, Petrov A, Choi J, Puglisi JD. 2017. Post-termination Ribosome Intermediate Acts as the Gateway to Ribosome Recycling. Cell Rep 20:161–172.

36. Zhu M, Dai X, Wang YP. 2016. Real time determination of bacterial in vivo ribosome translation elongation speed based on LacZalpha complementation system. Nucleic Acids Res 44:e155.

37. Dai X, Zhu M, Warren M, Balakrishnan R, Patsalo V, Okano H, Williamson J R, Fredrick K, Wang YP, Hwa T. 2016. Reduction of translating ribosomes enables Escherichia coli to maintain elongation rates during slow growth. Nat Microbiol 2:16231.

38. Naaktgeboren N, Roobol K, Voorma HO. 1977. The effect of initiation factor IF-1 on the dissociation of 70-S ribosomes of Escherichia coli. Eur J Biochem 72:49–56.

39. Ling C, Ermolenko DN. 2015. Initiation factor 2 stabilizes the ribosome in a semirotated conformation. Proc Natl Acad Sci U S A 112:15874–15879.

40. Margaliot M, Tuller T. 2012. On the steady-state distribution in the homogeneous ribosome flow model. IEEE/ACM Trans Comput Biol Bioinform 9:1724–1736.

41. Elvekrog MM, Walter P. 2015. Dynamics of co-translational protein targeting. Curr Opin Chem Biol 29:79–86.

42. Bernstein HD, Hyndman JB. 2001. Physiological basis for conservation of the

641 signal recognition particle targeting pathway in Escherichia coli. J Bacteriol
642 183:2187–2197.
643 43. Wickström D, Wagner S, Baars L, Ytterberg AJ, Klepsch M, van Wijk KJ,
644 Luirink J, de Gier JW. 2011. Consequences of depletion of the signal recognition
645 particle in Escherichia coli. J Biol Chem 286:4598–4609.
646 44. Lee HC, Bernstein HD. 2001. The targeting pathway of Escherichia coli
647 presecretory and integral membrane proteins is specified by the hydrophobicity
648 of the targeting signal. Proc Natl Acad Sci U S A 98:3471–3476.
649 45. Zhang D, Sweredoski MJ, Graham RL, Hess S, Shan SO. 2012. Novel
650 proteomic tools reveal essential roles of SRP and importance of proper
651 membrane protein biogenesis. Mol Cell Proteomics 11:M111.011585.
652 46. Scotti PA, Valent QA, Manting EH, Urbanus ML, Driessen AJ, Oudega B,
653 Luirink J. 1999. SecA is not required for signal recognition particle-mediated
654 targeting and initial membrane insertion of a nascent inner membrane protein. J
655 Biol Chem 274:29883–29888.
656 47. Weiss DS, Chen JC, Ghigo JM, Boyd D, Beckwith J. 1999. Localization of FtsI
657 (PBP3) to the septal ring requires its membrane anchor, the Z ring, FtsA, FtsQ,
658 and FtsL. J Bacteriol 181:508–520.
659 48. Jander G, Cronan J, Beckwith J. 1996. Biotinylation in vivo as a sensitive
660 indicator of protein secretion and membrane protein insertion. J Bacteriol
661 178:3049–3058.
662 49. Lee CA, Beckwith J. 1986. Suppression of growth and protein secretion defects

663 in Escherichia coli secA mutants by decreasing protein synthesis. J Bacteriol
664 166:878–883.
665 50. Hershey JW, Sonenberg N, Mathews MB. 2012. Principles of translational
666 control: an overview. Cold Spring Harb Perspect Biol 4:a011528.
667 51. Scott M, Gunderson CW, Mateescu EM, Zhang Z, Hwa T. 2010.
668 Interdependence of cell growth and gene expression: origins and consequences.
669 Science 330:1099–1102.
670 52. Laskowska E, Kuczyńska-Wiśnik D, Lipińska B. 2019. Proteomic analysis of
671 protein homeostasis and aggregation. J Proteomics 198:98–112.
672 53. Stein KC, Frydman J. 2019. The stop-and-go traffic regulating protein
673 biogenesis: How translation kinetics controls proteostasis. J Biol Chem
674 294:2076–2084.
675 54. Schibich D, Gloge F, Pohner I, Björkholm P, Wade R, von Heijne G, Bukau B,
676 Kramer G. 2016. Global profiling of SRP interaction with nascent polypeptides.
677 Nature 536:219–223.
678 55. Bornemann T, Jöckel J, Rodnina MV, Wintermeyer W. 2008. Signal sequence-
679 independent membrane targeting of ribosomes containing short nascent
680 peptides within the exit tunnel. Nat Struct Mol Biol 15:494–499.
681 56. Mohler K, Ibba M. 2017. Translational fidelity and mistranslation in the cellular
682 response to stress. Nat Microbiol 2:17117.
683 57. Phillips GJ, Silhavy TJ. 1992. The E. coli ffh gene is necessary for viability and
684 efficient protein export. Nature 359:744–746.

58. Kikuchi S, Shibuya I, Matsumoto K. 2000. Viability of an Escherichia coli pgsA null mutant lacking detectable phosphatidylglycerol and cardiolipin. J Bacteriol 182:371–376.

59. Gopalakrishnan AS, Chen YC, Temkin M, Dowhan W. 1986. Structure and expression of the gene locus encoding the phosphatidylglycerophosphate synthase of Escherichia coli. J Biol Chem 261:1329–1338.

60. Malecki M, Bárria C, Arraiano CM. 2014. Characterization of the RNase R association with ribosomes. BMC microbiology 14:34.

61. Quan S, Zhang N, French S, Squires CL. 2005. Transcriptional polarity in rRNA operons of Escherichia coli nusA and nusB mutant strains. J Bacteriol 187:1632–1638.

62. Wiśniewski JR, Mann M. 2012. Consecutive proteolytic digestion in an enzyme reactor increases depth of proteomic and phosphoproteomic analysis. Anal Chem. 84:2631–2637.

63. Wiśniewski JR, Zougman A, Nagaraj N, Mann M. 2009. Universal sample preparation method for proteome analysis. Nature Methods 6:359–362.

64. Tsolis KC, Economou A. 2017. Quantitative Proteomics of the E. coli Membranome. Methods Enzymol 586:15–36.

65. Jylhä A, Nättinen J, Aapola U, Mikhailova A, Nykter M, Zhou L, Beuerman R, Uusitalo H. 2018. Comparison of iTRAQ and SWATH in a clinical study with multiple time points. Clin Proteomics 15:24.

66. Callister SJ, Barry RC, Adkins JN, Johnson ET, Qian WJ, Webb-Robertson BJ,

Smith RD, Lipton MS. 2006. Normalization approaches for removing systematic biases associated with mass spectrometry and label-free proteomics. J Proteome Res 5:277–286.

67. O'Connor M, Thomas CL, Zimmermann RA, Dahlberg AE. 1997. Decoding fidelity at the ribosomal A and P sites: influence of mutations in three different regions of the decoding domain in 16S rRNA. Nucleic Acids Res 25:1185–1193.

68. Hecht A, Glasgow J, Jaschke PR, Bawazer LA, Munson MS, Cochran JR, Endy D, Salit M. 2017. Measurements of translation initiation from all 64 codons in E. coli. Nucleic acids research 45:3615–3626.

69. Dai X, Zhu M, Warren M, Balakrishnan R, Okano H, Williamson JR, Fredrick K, Hwa T. 2018. Slowdown of Translational Elongation in Escherichia coli under Hyperosmotic Stress. mBio 9:e02375-17.

70. Zarai Y, Margaliot M, Tuller T. 2013. Explicit expression for the steady-state translation rate in the infinite-dimensional homogeneous ribosome flow model. IEEE/ACM Trans Comput Biol Bioinform 10:1322–1328.

71. Zarai Y, Margaliot M, Tuller T. 2014. Maximizing Protein Translation Rate in the Ribosome Flow Model: The Homogeneous Case. IEEE/ACM Trans Comput Biol Bioinform 11:1184–1195.

72. Chen I, Howarth M, Lin W, Ting AY. 2005. Site-specific labeling of cell surface proteins with biophysical probes using biotin ligase. Nat Methods 2:99–104.

729 **FIGURES**

730
731
732
733
734
735
736
737

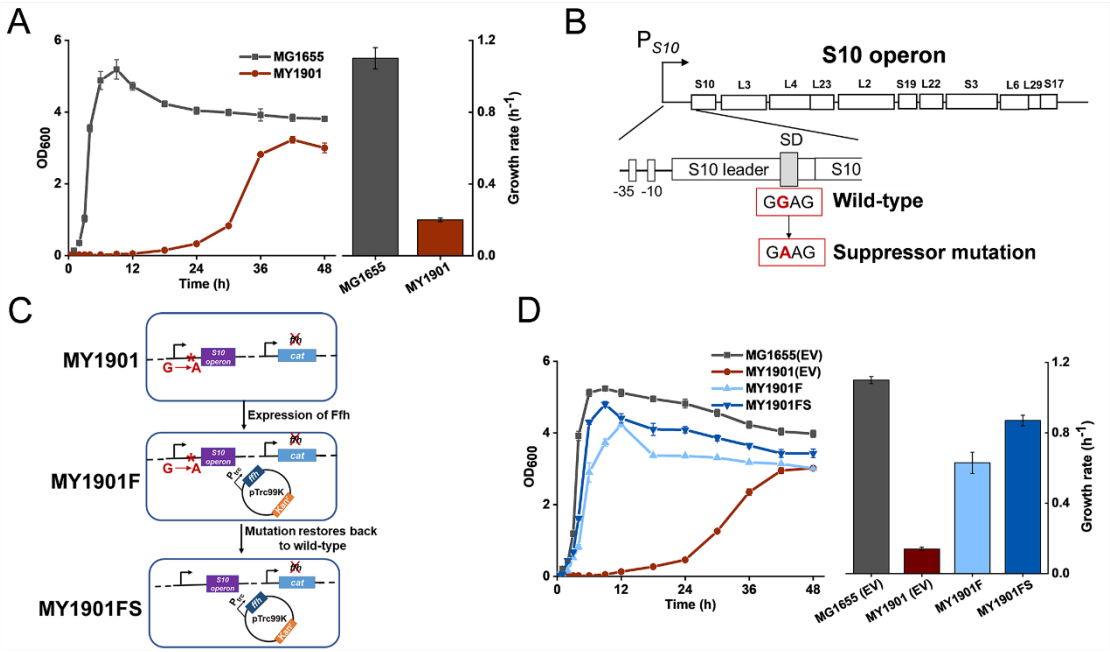

738 **FIG 1** Isolation SRP suppressor strain and its growth. (A) Growth curves and growth
739 rates of wild-type strain MG1655 and suppressor strain MY1901. (B) The suppressor
740 mutation sites in the SD sequence of S10 operon. The region and encoded ribosomal
741 proteins of the S10 operon are shown. The wild-type SD sequence (GGAG) mutated
742 into suppressor mutation (GAAG). (C) Restoration of the wild-type alleles. Plasmid
743 pTrc99K-Ffh was first transformed into strain MY1901, generating the strain MY1901F.
744 Ffh protein was expressed with the basal level in MY1901 to reduce the toxicity of
745 overexpression of Ffh. Then, the suppressor mutation (GAAG) was restored to wild-
746 type SD sequence (GGAG) by site-directed mutagenesis, generatiing the strain
747 MY1901FS. (D) Growth curves and growth rates of strains restored to the wild-type.
748 Strains MG1655 and MY1901 carrying the empty vector (EV) pTrc99K were used as
749 control. Solid curves are the mean of three independent measurements and error bars
750 represent the standard error of the mean of samples. Growth rates were figured out from

751 the exponential growth phase. All growth rates shown represent the mean growth rates

752 from three biological replicates, and error bars represent the standard error of the mean

753 value.

754

755

756

757

758

759

760

761

762

763

764

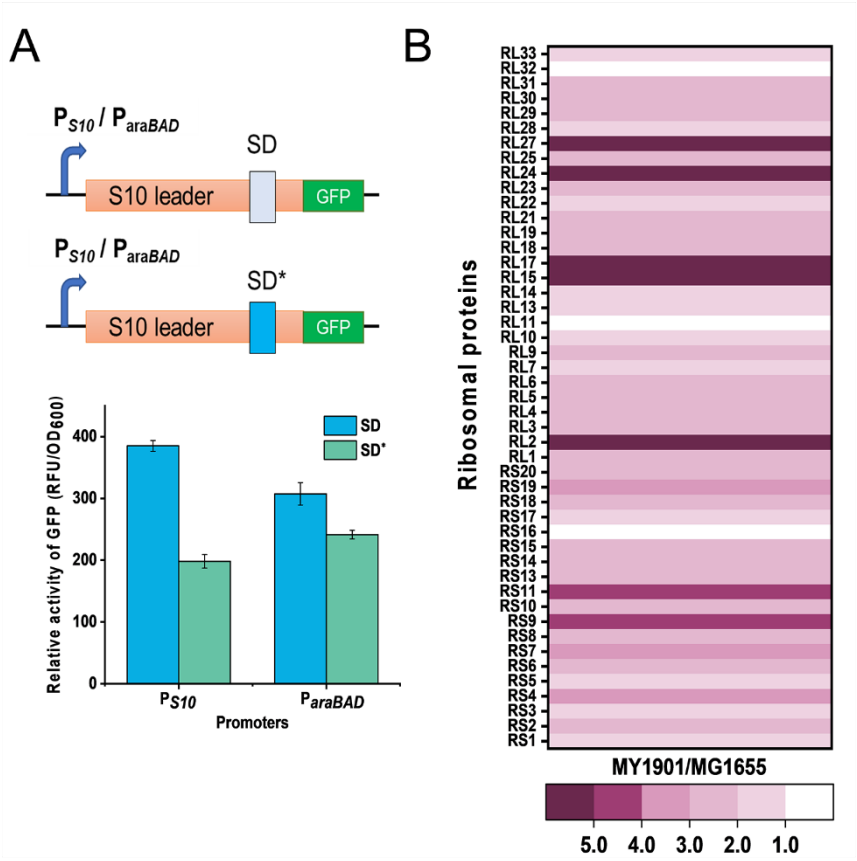

765 **FIG 2** Effects of SRP suppressor on ribosomal protein synthesis. (A) Effect of mutant

766 SD sequence on protein translation. GFP was used as a reporter to measure gene

767 expression. (Top) Graphical representation of GFP expression. P_{S10} / P_{araBAD} -GFP with

768 wild-type SD and suppressor mutation SD* were introduced into cells. (Bottom)

769 Fluorescence measurement of GFP. Data represent the mean of six independent

770 experiments, and error bars represent the standard error of the mean value. (B) Fold

771 changes in the expression of ribosomal proteins in strain MY1901relative to that in

772 strain MG1655 (Data set S1B).

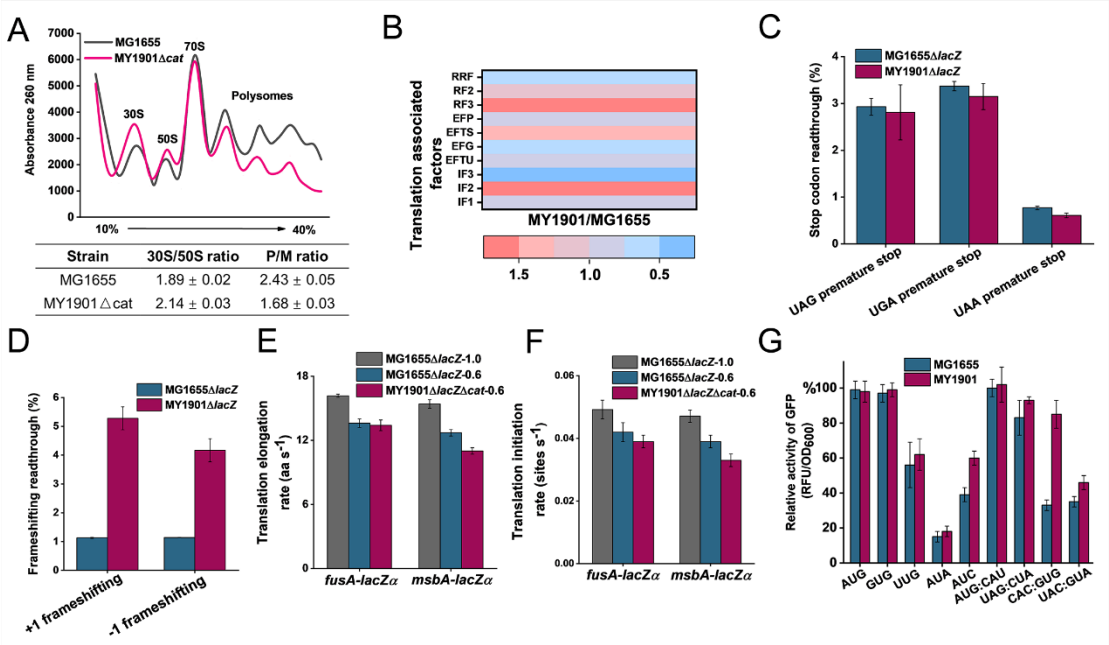

FIG 3 Effects of SRP suppressor on translation efficiency. (A) Polysome profiles of wild-type strain MG1655 and suppressor strain MY1901Δ*cat*. Data represent the mean ± SEM of three independent experiments. (B) Fold changes in the expression of translation associated factors in strain MY1901relative to that in strain MG1655 (Data set S1B). (C-D) Effect of suppressor mutation on stop-codon (C) and frameshifting (D) readthrough. β-galactosidase activities of strains harboring the mutant LacZ reporters were calculated relative to that of the same strain harboring the wild-type LacZ. (E)The translation elongation rates of FusA-LacZα and MsbA-LacZα under different growth rates (MG1655Δ*lacZ*, 1.0 h^{-1}; MG1655Δ*lacZ*, 0.6 h^{-1}; MY1901Δ*lacZ*Δ*cat*, 0.6 h^{-1}). (F) Translation initiation rates of proteins were estimated based on their corresponding translation elongation rates. (G) Initiation with various non-canonical start codons and non-initiator tRNAs codons in the wild-type and suppressor strains. Relative activities of mutant GFP were calculated relative to that of the same strain harboring the wild-type GFP. The wild-type start codon was indicated as AUG and the wild-type initiator

tRNA was indicated as AUG: CAU. All data are averages of six independent experiments, and error bars represent the SEM value.

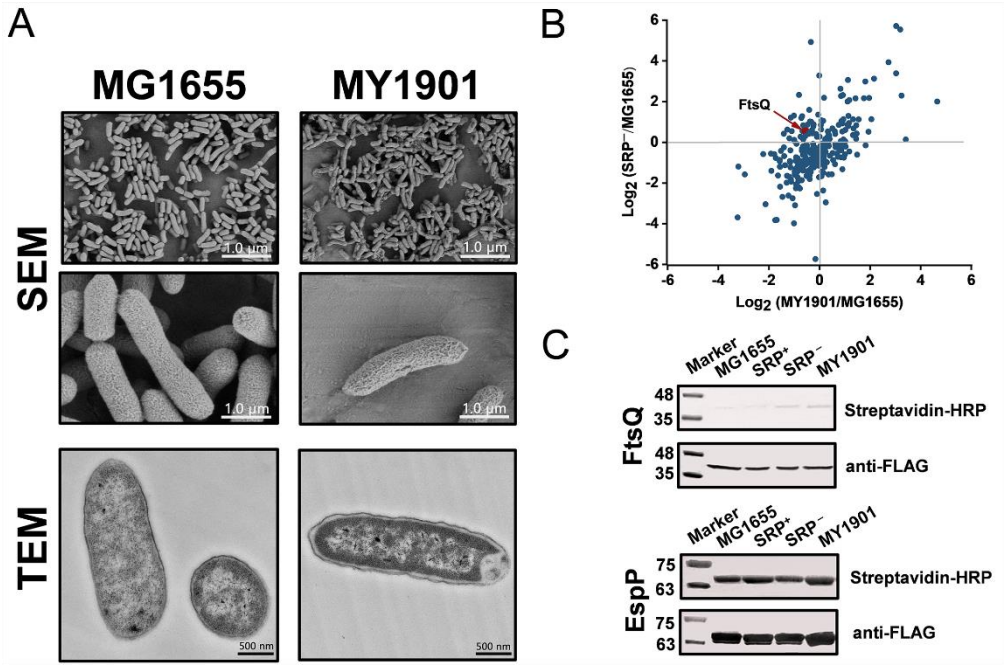

FIG 4 Suppressor mutation suppresses targeting defects of partial inner membrane proteins. (A) Scanning electron microscopy (SEM) and transmission electron microscopy (TEM) analysis of wild-type strain MG1655 and suppressor strain MY1901. For SEM, the scale bar is 1.0 μm. For TEM, the scale bar is 500 nM. (B) Quantification of identified SRP-dependent inner membrane proteins in strains MY1901 and SRP^{-} (Data set S1D). Protein abundance of MY1901 and SRP^{-} is relative to that of wild-type MG1655. (C) FtsQ (left) and EspP (right) targeting assay by their biotinylation. SRP^{+}, Ffh expression in HDB51 strain; SRP^{-}, Ffh depletion in HDB51 strain.

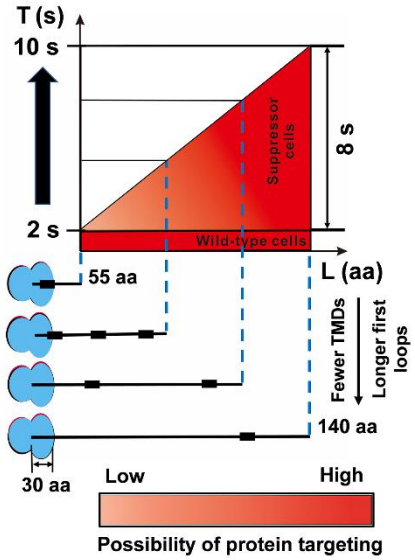

FIG 5 The SRP suppressor extends the time window for protein targeting. In wild-type MG1655 cells, although the critical length (L) of inner membrane proteins is variable, the targeting time (T) is fast (~2 s). The suppressor cells with a slower elongation rate extended the time window for protein targeting to 2-10 s. For details and references, see Discussion.